Rheological characterization of complex dynamics in Na–Zn metaphosphate glass-forming liquids

Cite as: J. Chem. Phys. **155**, 054503 (2021); https://doi.org/10.1063/5.0060360 Submitted: 17 June 2021 • Accepted: 18 July 2021 • Published Online: 03 August 2021

Yiqing Xia, Hao Chen, Bruce Aitken, et al.







riqing Ala, riao Chen, Brace Aitken, et al.

ARTICLES YOU MAY BE INTERESTED IN

Dynamical crossover and its connection to the Widom line in supercooled TIP4P/Ice water The Journal of Chemical Physics 155, 054502 (2021); https://doi.org/10.1063/5.0059190

Theory of the effect of external stress on the activated dynamics and transport of dilute penetrants in supercooled liquids and glasses

The Journal of Chemical Physics 155, 054505 (2021); https://doi.org/10.1063/5.0056920

Quantifying dynamical and structural invariance in a simple molten salt model
The Journal of Chemical Physics 155, 054506 (2021); https://doi.org/10.1063/5.0055794





Rheological characterization of complex dynamics in Na-Zn metaphosphate glass-forming liquids

Cite as: J. Chem. Phys. 155, 054503 (2021); doi: 10.1063/5.0060360

Submitted: 17 June 2021 • Accepted: 18 July 2021 •

Published Online: 3 August 2021







Yiqing Xia, Hao Chen, Bruce Aitken, and Sabyasachi Sen la

AFFILIATIONS

- Department of Materials Science and Engineering, University of California at Davis, Davis, California 95616, USA
- ²Science and Technology Division, Corning Inc., Corning, New York 14831, USA
- a) Author to whom correspondence should be addressed: sbsen@ucdavis.edu

ABSTRACT

The viscoelastic behavior and shear relaxation in supercooled $[NaPO_3]_x[Zn(PO_3)_2]_{1-x}$ metaphosphate liquids with $0.2 \le x \le 1.0$ are investigated using a combination of small amplitude oscillatory and steady shear parallel plate rheometry, resonant ultrasound spectroscopy, and differential scanning calorimetry. The results demonstrate that these liquids are thermorheologically complex with the coexistence of a fast and a slow relaxation process, which could be attributed to the segmental motion of the phosphate chains and the Zn–O bond scission/renewal dynamics, respectively. The segmental motion of the phosphate chains is found to be the dominant process associated with the shear relaxation for all metaphosphate liquids. The compositional evolution of the calorimetric fragility of these liquids is shown to be related to the conformational entropy of the constituent phosphate chains, which is manifested by the width of the relaxation time distribution for the segmental chain motion. This entropy decreases and the temporal coupling between the chain dynamics and Zn–O bond scission-renewal increases with the increasing Zn content as the higher field strength Zn modifier ions provide more effective cross-linking between the phosphate chains.

Published under an exclusive license by AIP Publishing. https://doi.org/10.1063/5.0060360

I. INTRODUCTION

The technological importance of phosphate glasses originates primarily from their unique properties, including large composition range for glass formation, low glass transition temperature T_g , large solubility of rare earth and other high-field strength cations, high thermal expansion coefficient, and strong bioactivity. ^{1–9} Consequently, the atomic structure–property relationships in these glasses have been investigated in detail over the last few decades. ^{10–15} However, in comparison, relatively little is known regarding the structural control on the viscoelastic behavior of the parent supercooled liquids from which these glasses are derived. The viscoelastic behavior of a supercooled glass-forming liquid is intimately linked to the material's viability for all stages of industrial processing, including melting, forming, and annealing, and, therefore, is of key significance in the optimization of corresponding processing parameters. ¹⁶

Analyses of the temperature-dependent viscosity data $\eta(T)$ of alkali phosphate liquids with ≥ 50 mol.% P_2O_5 available in the literature have shown that the fragility index $m = \frac{d \log \eta(T)}{d(T_g/T)}\Big|_{T=T_g}$ is

a sensitive function of the structural connectivity $\langle n \rangle$ of the phosphate network, where $\langle n \rangle$ is defined as the average number of bridging oxygen per PO₄ tetrahedron in the glass structure, which varies from 2 in metaphosphates with 50% P₂O₅ to 3 in pure P₂O₅. ^{17,18} The phosphate network of alkali metaphosphate liquids is characterized predominantly by chains of corner-sharing PO₄ tetrahedra, and the high conformational entropy of these chains is believed to be responsible for the relatively high fragility ($m \sim 80$) of these liquids.¹⁹ As (n) increases on progressive addition of P₂O₅, these chains get increasingly cross-linked and the conformational entropy of the network decreases with a concomitant lowering of *m*. Finally, m reaches its minimum value of ~ 20 as $\langle n \rangle$ becomes 3 for pure P_2O_5 . Strong similarity in the variation of m with $\langle n \rangle$ among different alkali phosphate liquids suggests that shear relaxation and viscous flow in these liquids are primarily controlled by the phosphate network, which is only weakly coupled to the modifier ions. On the other hand, recent studies have shown that *m* can vary over a rather large range spanning from ~30 to 90 as a function of the field strength of the modifier cation even in metaphosphate liquids with the same nominal connectivity of the phosphate network. 19,20

Metaphosphates with high field strength modifier cations, such as alkaline-earths and Zn, are characterized by low m, while those with low-field strength modifiers, such as alkalis and Ag, are characterized by rather large m. This variation was hypothesized to be related to the fact that the extent and the strength of the effective cross-linking of the phosphate chains by the modifier cation—oxygen polyhedra in the structure of metaphosphate liquids increase with the increasing field strength of the modifiers. ¹⁹ Such a role of the modifier cation in controlling the fragility of metaphosphates is clearly demonstrated by the variation of m along the Na–Zn metaphosphate join, where m decreases monotonically from ~70 for the Na-metaphosphate to ~28 for the Zn-metaphosphate. ²¹

Recent rheological and variable-temperature ³¹P magic-anglespinning nuclear magnetic resonance (MAS NMR) spectroscopic studies have indicated that, similar to low molecular weight chain polymers, the viscous flow and shear relaxation of the highly fragile Ag-metaphosphate liquid are closely associated with the segmental motion of constituent phosphate chains.²² Additionally, this liquid was found to be thermorheologically complex, violating time-temperature superposition (TTS). In contrast, the shear relaxation of phosphate networks with higher degree of connectivity, such as ultraphosphates, appears to be controlled by chemical exchange between the constituent PO₄ species via P-O bond scission-renewal dynamics.^{23,24} Interestingly, an analogous transition from fragile liquids with shear relaxation controlled by segmental Se chain motion to strong liquids with relaxation predominantly controlled by bond scission-renewal dynamics was observed in binary As-Se liquids with the addition of As resulting in progressive cross-linking of Se chains.^{25,26} However, it remains to be seen whether a similar transition in the shear relaxation mechanism can also be observed in metaphosphate liquids with a progressive increase in the effective crosslinking of the phosphate chains as a low field strength modifier cation (e.g., Na) is replaced by a high field strength one (e.g., Zn). 19,27 Here, we report the results of a detailed rheological study of the viscoelastic properties and the shear relaxation behavior of [NaPO₃]_x[Zn(PO₃)₂]_{1-x} supercooled liquids with varying Na:Zn ratios using a combination of small amplitude oscillatory shear (SAOS) and calorimetric measurements. The relationships between fragility, structure, and the various relaxational modes and their timescale distributions in these liquids are established.

II. EXPERIMENTAL METHODS

A. Sample preparation and physical characterization

The $[NaPO_3]_x[Zn(PO_3)_2]_{1-x}$ metaphosphate glasses were prepared by the conventional melt-quenching method. Appropriate amounts of $NH_4H_2PO_4$ (99.9%, Acros Organics), Na_2CO_3 (ACS grade, MilliporeSigma), and ZnO (99.99%, Alfa Aesar) were mixed and loaded in a quartz crucible. The mixtures were first calcined at $450\,^{\circ}\text{C}$ for 17 h to remove any water and ammonia. Subsequently, the calcined batches were melted at $1100\,^{\circ}\text{C}$ for 1 h. These melts were then quenched onto a graphite plate. Resulting glass samples were immediately transferred into a desiccator for storage to avoid exposure to atmospheric moisture.

The T_g of these Na–Zn metaphosphate glasses was determined using differential scanning calorimetry (Mettler Toledo DSC1). Samples of mass ~15–25 mg were taken in hermetically sealed Al pans and heated at a rate of 10 K/min in a flowing nitrogen

environment above T_g to remove thermal history. The fictive temperature T_f was taken as the peak of the endothermic glass transition signal while heating the sample at a specific rate q K/min ranging from 0.5 to 30 K/min, subsequent to cooling at the same rate from $T_g + 30$ K to $T_g - 50$ K. T_g was determined to be within ± 2 °C as the onset of the glass transition endotherm at a heating rate of 10 K/min. The fictive temperature T_f of $[NaPO_3]_x[Zn(PO_3)_2]_{1-x}$ liquids was determined as a function of the heating rate q varying from 0.5 to 30 K/min, following the method of Wei et al., and the fragility index m was subsequently determined from the activation energy E of enthalpy relaxation according to the relation $m = \frac{E}{pT_0} \frac{28,29}{10.10}$

Density of these glasses was measured using a gas expansion pycnometer (Micromeritics AccuPyc II 1340) at 20 °C using helium (6N purity) as the displacement gas. For each measurement, ~0.5 g of the glass sample was loaded into a 1 cm³ cup. All reported density values are averages of ten consecutive measurements of each sample. The shear modulus of these samples was determined at room temperature using a resonant ultrasound spectrometer (ACE-RUS008). The resonant ultrasound spectroscopy (RUS) technique uses the free-body mechanical resonances of approximately mm sized samples to determine their complete elastic modulus matrix. Each glass sample was cut into a rectangular parallelepiped geometry (\sim 7 × 5 × 3 mm³), and the surfaces were polished flat and parallel. The as-prepared sample was mounted on opposing corners between two piezoelectric transducers. In the RUS system, an elastic wave of constant amplitude and varying sweeping frequency is generated by the drive transducer, and the corresponding resonances are measured by the pickup transducer. The resonant frequency spectra in the frequency range between 50 and 400 kHz were measured. The resonances were subsequently fitted to Lorentzian peaks, and the RUS frequency data were analyzed using the Lagrangian minimization code developed at the Los Alamos National Laboratory in conjunction with the mass density of the sample to obtain the elastic moduli. More details on the RUS experiments and data analysis can be found in the literature. 30,31

B. Parallel plate rheometry

The viscoelastic behavior of the [NaPO₃]_x[Zn(PO₃)₂]_{1-x} metaphosphate liquids was measured using a parallel plate rheometer (MCR 302, Anton Paar) under oscillatory shear mode in an environment of flowing nitrogen gas. In this rheometer, the temperature was controlled by a convection oven. Before the rheometry measurements, the glass samples were heated above the softening point to reach a viscosity of $\sim 10^5$ Pa s and trimmed between the two plates to form a sandwich-like geometry with a gap of ~1 mm. At each desired measurement temperature, the samples were allowed to equilibrate for 5 min followed by the application of a sinusoidal strain with varying angular frequency ω between 1 and 628 rad/s and the induced torque was recorded to calculate the storage and loss moduli G'and G'' as a function of ω . The upper plate (8 mm diameter, stainless steel) was used to apply the sinusoidal strain, while the non-removable lower plate (25 mm diameter, stainless steel) remained stationary. The corresponding stress response was recorded using a torque transducer. The applied strain of all oscillatory shear measurements was controlled within a predetermined linear viscoelastic region. Master curves of G' and G'' were obtained

using time–temperature superposition (TTS) where the vertical shift factor was found to be nearly independent of temperature and to vary between 0.75 and 1.25 for all compositions. The systematic errors for G' and G'', introduced by the torsional instrument compliance, were considered and corrected using the following equations:³²

$$G_c' = \frac{G_m' \left(1 - \frac{J_i}{k_g} G_m'\right) - \frac{J_i}{k_g} {G_m''}^2}{\left(1 - \frac{J_i}{k_g} G_m'\right)^2 + \left(\frac{J_i}{k_e} G_m''\right)^2},\tag{1}$$

$$G_c'' = \frac{G_m''}{\left(1 - \frac{J_i}{k_c} G_m'\right)^2 + \left(\frac{J_i}{k_c} G_m''\right)^2},\tag{2}$$

where G_c' and G_c'' denote the corrected storage modulus and loss modulus values, respectively, while G_m' and G_m'' are the measured values. J_i is the torsional instrument compliance, and k_g is the geometry factor given by $k_g = \frac{2h}{\pi R^4}$, where h is the sample thickness and R is the plate radius (4 mm). The instrument compliance of the rheometer setup was measured by the gluing method where the upper (8 mm, stainless steel) and lower plates (25 mm, stainless steel) were fixed together with a very thin layer (<20 μm) of cyanoacrylate glue.³³ After 24h drying time, a torque sweep was carried out to measure the corresponding deflection angle and the slope of the corresponding linear relationship was used to determine the instrument compliance J_i to be 0.000715 rad/N m. All reported G' and G'' data in this work are corrected values. The Newtonian viscosity of the $[NaPO_3]_{0.8}[Zn(PO_3)_2]_{0.2}$ liquid in the range $\sim 10^5 - 10^8$ Pa s was measured using steady shear, where the viscosity was determined as the ratio of stress and strain rate at various shear rates $\dot{\gamma}$ ranging between 0.01 and 1 s⁻¹ at each temperature. More details on the rheometry experiments and data processing can be found in previous publications.34,35

III. RESULTS AND DISCUSSION

The T_g of the $[NaPO_3]_x[Zn(PO_3)_2]_{1-x}$ metaphosphate glasses measured in this study displays a nonlinear compositional variation as it steeply decreases with the initial replacement of Zn with Na as x increases from 0 to 0.2, beyond which a more gradual linear decrease is observed for $0.2 \le x \le 1.0$ (Fig. 1). Such a variation is consistent with the expectation that the lower field strength of the Na cations compared to that of Zn would result in weaker effective cross-linking of the constituent phosphate chains. In this scenario, the sharp drop in T_g with the initial addition of Na to up to x = 0.2 is likely indicative of the percolation of these weakly linked regions in the glass structure. The increasingly weaker interchain coupling upon progressive replacement of Zn with Na in these metaphosphate glasses is also evident in the compositional variation of the shear modulus G, which displays a sharp drop from ~19 to ~7 GPa as x increases from 0 to 0.6 (Fig. 2). A further increase in Na content results in a negligible change in G. On the other hand, the molar volume of these $[NaPO_3]_x[Zn(PO_3)_2]_{1-x}$ glasses decreases in a linear fashion with x over the entire composition range implying a corresponding increase in the atomic packing (Fig. 3). The highest molar volume of the Zn(PO₃)₂ glass may be indicative of an open tetrahedral network of corner shared ZnO₄ and PO₄ tetrahedra.

The master plots of the ω dependence of G' and G'' of all $[NaPO_3]_x[Zn(PO_3)_2]_{1-x}$ supercooled liquids investigated in this

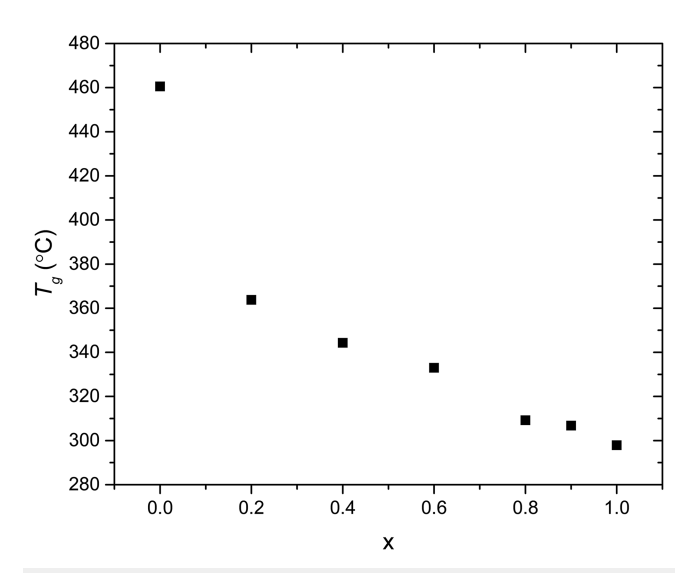


FIG. 1. Glass transition temperature of $[NaPO_3]_x[Zn(PO_3)_2]_{1-x}$ glasses obtained in this study. Experimental uncertainties are within the size of the symbols.

study obtained by performing TTS at an iso-viscous ($\sim 10^7$ Pa s) temperature are shown in Fig. 4. Although TTS is not strictly obeyed by these liquids (see below), here we have approximated TTS solely for the convenience of visualization of the data over the entire frequency range, and therefore the master curves shown in Fig. 4 should be treated as only approximate. It can be observed that, in the low frequency viscous regime, G' and G'' follow the Maxwell scaling of $\sim \omega^2$ and $\sim \omega$, respectively, while with increasing ω beyond the G'-G'' crossover, G' reaches the glassy plateau

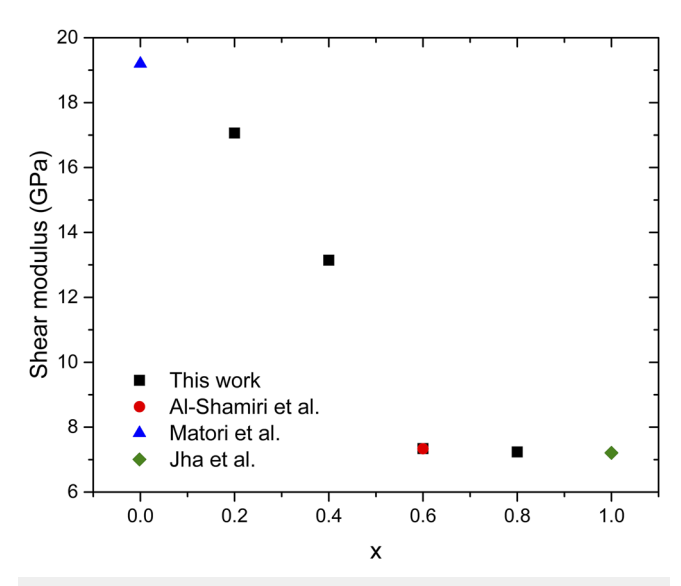


FIG. 2. Shear modulus of $[NaPO_3]_x[Zn(PO_3)_2]_{1-x}$ glasses measured in the present study (black squares). Results reported by Al-Shamiri and Eid⁴⁵ (red circle), Matori *et al.*⁴⁶ (blue triangle), and Jha *et al.*⁴⁷ (green diamond) are shown for comparison. Experimental uncertainties are within the size of the symbols.

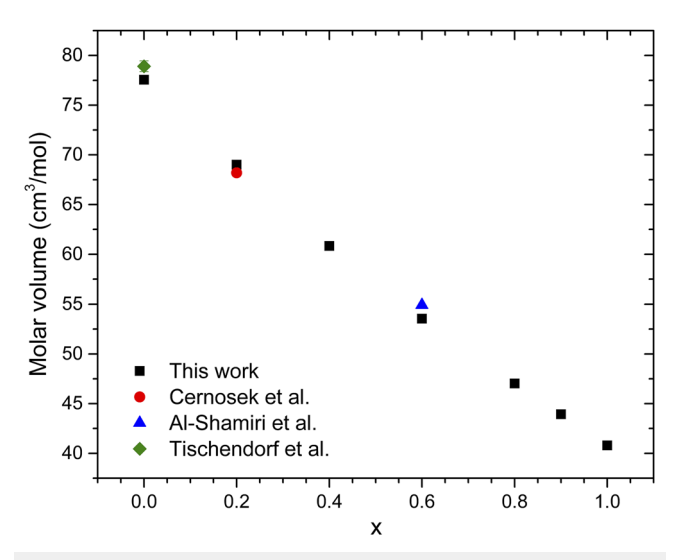


FIG. 3. Molar volume of [NaPO₃]_x[Zn(PO₃)₂]_{1-x} glasses measured in the present study (black squares). Results reported by Černošek *et al.*⁴⁸ (red circle), Al-Shamiri and Eid⁴⁵ (blue triangle), and Tischendorf *et al.*⁴⁹ (green diamond) are shown for comparison. Experimental uncertainties are within the size of the symbols.

value of G_{∞} (~10 GPa) and G'' decreases. The G_{∞} values of these liquids thus obtained are found to be consistent with the shear modulus of the corresponding glasses determined at ambient temperature by RUS measurements, which validates the torsional instrument compliance correction methodology adopted in this study. Perhaps most interestingly, the frequency dependence of G' changes from the Maxwell scaling of $\sim \omega^2$ in the terminal regime to a nearly linear scaling of $\sim \omega^1$, which continues until the crossover of \dot{G} and G''. Such a scaling behavior has been reported in the literature for several supramolecular polymeric liquids that consist of short chains of a few molecules as well as for As-Se and Agmetaphosphate liquids with short Se or phosphate chains, respectively, and, hence, can be ascribed to the chain reorientation dynamics in these liquids. 19,26,36,37 Further insight into the viscoelastic relaxation process in these Na-Zn metaphosphate liquids can be obtained from the van Gurp-Palmen (vGP) plot (Fig. 5) of the phase angle $\delta = \tan^{-1}(G''/G')$ vs the absolute value of the complex modulus $|G^*| = \sqrt{G'^2 + G''^2}$ at various temperatures.³⁸ If a glass-forming liquid is strictly thermorheologically simple, i.e., it obeys TTS, the vGP plots at different temperatures are expected to overlap with each other to form a single curve. It is clear from Fig. 5 that such thermorheological simplicity is violated for all [NaPO₃]_x[Zn(PO₃)₂]_{1-x} supercooled liquids, and especially for those with x > 0.2, which is indicative of the existence of multiple relaxation processes with different activation energies. As noted above, at least two major dynamical processes have been associated in the past with the relaxation of phosphate liquids, one of which is a reorientation or a segmental motion of the constituent chains and the other involves P-O bond scission/renewal.^{22–24} This scenario is then consistent with the observed violation of thermorheological simplicity in the Na-Zn metaphosphate liquids. In addition, it is apparent from Fig. 5 that the degree of this violation, i.e., the degree of thermorheological

complexity, increases with increasing Na:Zn ratio in these liquids. In Zn-rich compositions, the high degree of thermorheological simplicity is the manifestation of strong inter-chain cross-linking imparted by the high field strength Zn cations, which results in a mechanistic coupling between the chain motion and the P-O and/or Zn-O bond scission/renewal, with both processes likely being characterized by similar activation energies. On the other hand, with the increasing Na:Zn ratio, the metaphosphate chains in these liquids become less dynamically constrained and can perform facile segmental motion without direct assistance from bond scission/renewal. Consequently, the two relaxation processes become decoupled with different activation energies, which gives rise to the observed enhancement of thermorheological complexity in Na-rich compositions. In the extreme case of Na-metaphosphate, the PO₄ tetrahedral chains are the least constrained and the motion of Na ions are strongly decoupled from the structural network. This scenario is corroborated by the fact that the ionic conductivity near T_g of NaPO₃ glass is over four orders of magnitude higher than that of Zn(PO₃)₂ glass,²¹ which suggests a significantly weaker coupling between the modifier cation and the phosphate network in the former.

This hypothesis is further supported by the relaxation time spectra $H(\tau)$ of these Na–Zn metaphosphate supercooled liquids (Fig. 6) that were calculated from the $G'(\omega)$ data using the following relation proposed by Ferry:³⁹

Harmon proposed by Perry.
$$H(\tau) = \frac{G'(a\omega) - G'(\omega/a)}{2 \ln a} - \frac{a^2}{(a^2 - 1)^2} \times \frac{G'(a^2\omega) - G'(\omega/a^2) - 2G'(a\omega) + 2G'(\omega/a)}{2 \ln a} \bigg|_{1/\omega = \tau},$$
(3)

where a is the frequency interval on a logarithmic frequency scale of the measured $G'(\omega)$ values. As expected from the observed thermorheological complexity exhibited by the vGP plots (Fig. 5), the relaxation spectra $H(\tau)$ of all liquids can be simulated with two Gaussian components corresponding to two relaxation processes with overlapping timescale distributions (Fig. 6). Following the previously reported analyses of the $H(\tau)$ spectra of Se-rich As–Se and P-Se liquids, 40,41 the broad and intense component peak at short timescale in Fig. 6 is assigned to the segmental motion of the PO₄ tetrahedral chains, while the weak and narrow component peak at longer timescale is ascribed to the bond scission/renewal dynamics. As the relative peak intensity is determined by the probability of the relaxation mechanism, the relatively strong intensity of the broad peak in Fig. 6, which increases upon progressive replacement of Zn with Na, reflects the predominance of the segmental motion of phosphate chains in controlling the viscous flow and shear relaxation of metaphosphate liquids.²² This result is consistent with the hypothesis that the weak inter-chain cross-linking in Na-rich compositions gives rise to a lowering of dynamical constraints on chain reorientation. On the other hand, the narrow peak corresponding to the slow process increases in intensity with the increasing Zn:Na ratio. This result suggests that the slow process likely corresponds to the Zn-O bond scission/renewal, which becomes increasingly important as a constraint on chain reorientation.

It was shown in a previous rheological study of supercooled Se-rich P–Se liquids that the width of the timescale distribution

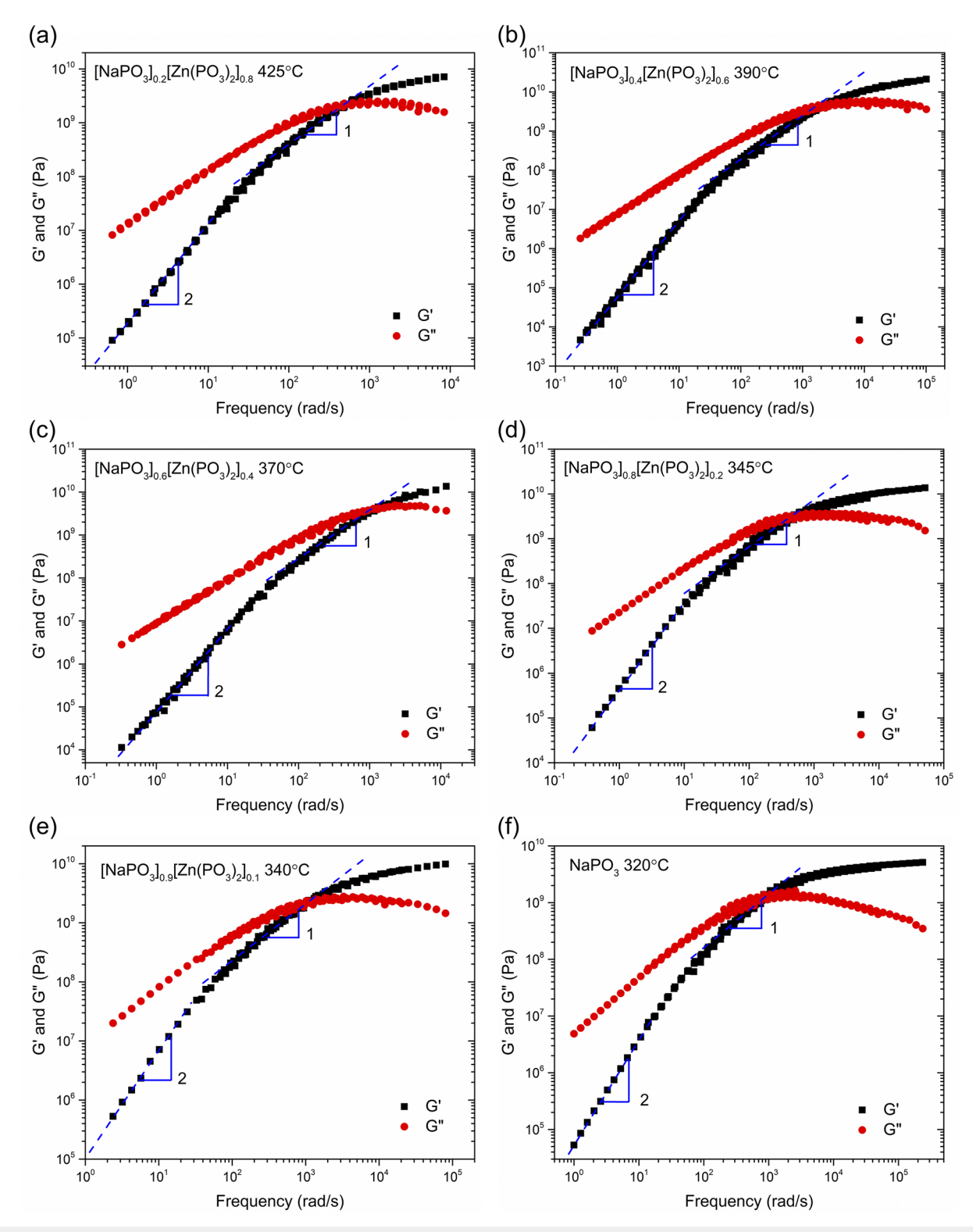


FIG. 4. (a)–(f) Master plots of angular frequency dependence of storage modulus G' (black squares) and loss modulus G'' (red circles) for $[NaPO_3]_x[Zn(PO_3)_2]_{1-x}$ liquids. The TTS reference temperature is listed alongside each composition. Blue dashed lines show frequency scaling of G' changing from $\sim \omega^2$ in the low frequency region to $\sim \omega^1$ at higher frequencies.

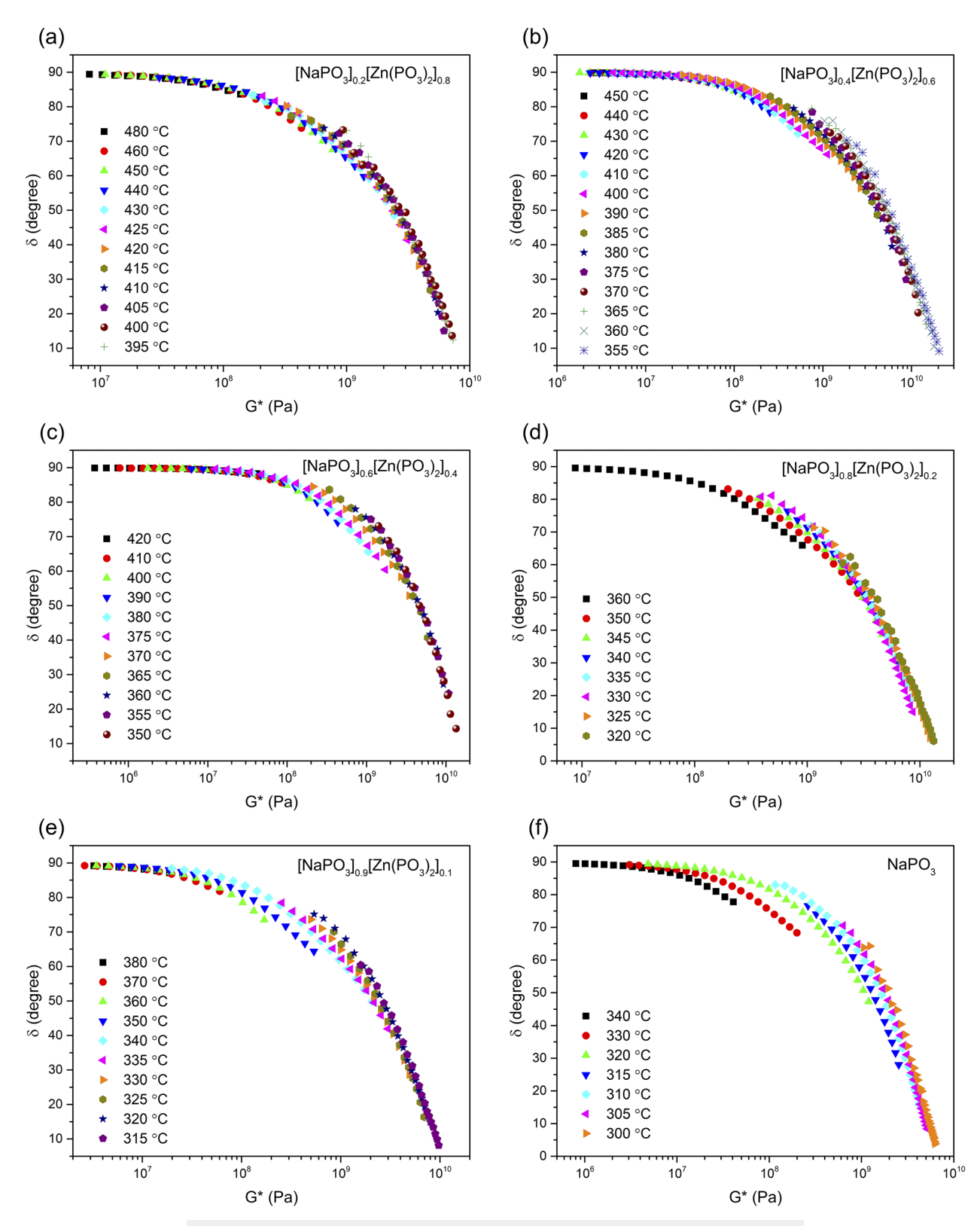


FIG. 5. (a)–(f) The van Gurp–Palmen plot of the phase angle δ vs G^* for [NaPO₃]_x[Zn(PO₃)₂]_{1-x} liquids.

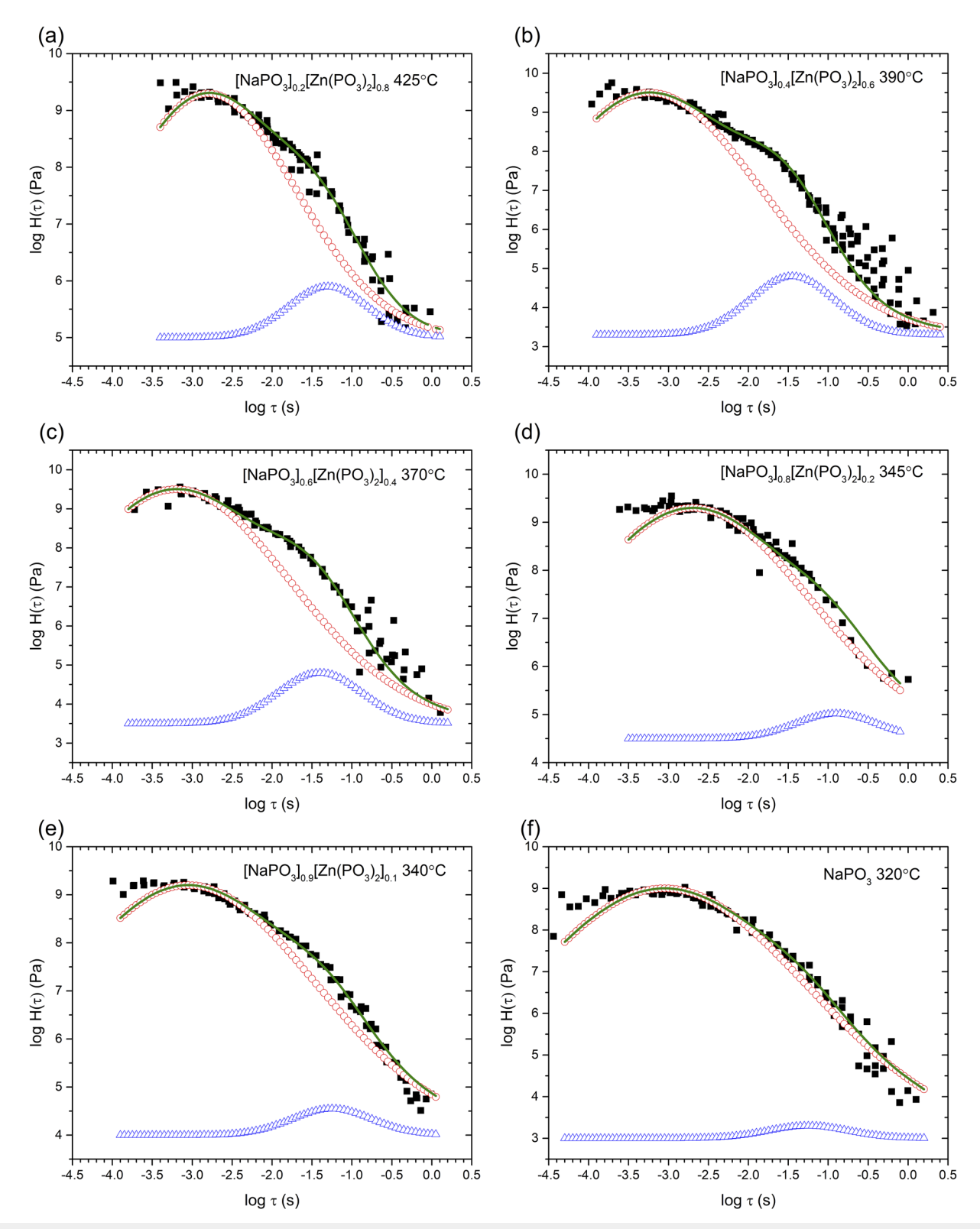


FIG. 6. (a)–(f) Relaxation spectra $H(\tau)$ of $[NaPO_3]_x[Zn(PO_3)_2]_{1-x}$ liquids. Filled squares are experimental data. Open circles and triangles represent the Gaussian components corresponding to the fast and slow processes, respectively. Solid lines represent the total fit to the experimental data.

for the segmental Se chain motion reflects the associated conformational entropy S_{conf} of the constituent chains and, thus, would be a sensitive function of the effective chain length.⁴¹ Additionally, the fragility index m of a wide variety of inorganic glass-forming network liquids, including phosphates, has been related in the past to the average connectivity $\langle r \rangle$ of the network through the relation $m^* \propto \left(\frac{dS_{conf}}{d(r)}\right)^2$, where $m^* = \frac{m - m_0}{m_0}$ is the reduced fragility index normalized with respect to a minimum fragility index $m_0 = 17$ and the term $\frac{dS_{conf}}{d(r)}$ can be taken to represent the change in the conformational entropy of chains upon increase in $\langle r \rangle$ due to progressive cross-linking.¹⁸ Therefore, the effective length of the metaphosphate chains or their effective degree of cross-linking, the reduced fragility index m^* , and the corresponding peak full-width-at-halfmaximum (FWHM) of the fast relaxation process in the $H(\tau)$ spectra of these Na-Zn metaphosphate liquids should be qualitatively correlated. The compositional dependence of the FWHM of this peak (Fig. 7) in these liquids is observed to increase from ~2.7 to ~4.2 log units upon increasing the Na:Zn ratio. The average phosphate chain length is estimated to be ~100-200 PO₄ tetrahedra for metaphosphate liquids^{22,42} and is likely somewhat shorter in Znmetaphosphate than in Na-metaphosphate due to the greater extent of Q-species disproportionation in the former. 43,44 However, the effective chain length in alkali-zinc metaphosphate glasses is likely to be controlled by the interaction between the phosphate chains and the modifier cations. The stronger cross-linking of the metaphosphate chains via Zn-O polyhedra in Zn-rich compositions would likely have a pinning effect on the chain reorientation and result in an effective shortening of the chain length, consistent with the observed compositional evolution of the FWHM of the $H(\tau)$ peak for the segmental chain dynamics (Fig. 7). This hypothesis is also supported by the compositional variation of the fragility index mof these Na-Zn metaphosphate liquids. The m value, determined calorimetrically in the present study, increases monotonically with

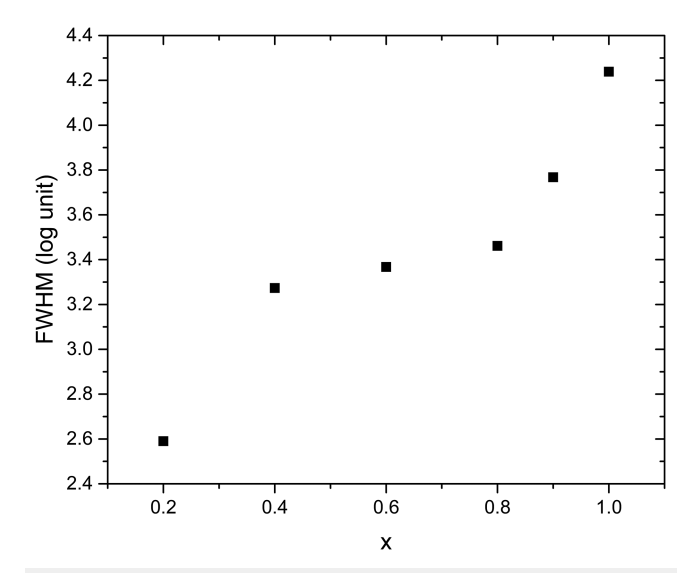


FIG. 7. FWHM of the Gaussian component corresponding to segmental chain motion in relaxation spectra $H(\tau)$ of $[NaPO_3]_x[Zn(PO_3)_2]_{1-x}$ supercooled liquids.

the increasing Na:Zn ratio (Fig. 8). Indeed, as expected from the above discussion, the corresponding reduced fragility indices m^* display an intriguing correlation with the corresponding variation in the FWHM of the fast relaxation process in the $H(\tau)$ spectra of these Na–Zn metaphosphate liquids (Fig. 8). In contrast, the FWHM of ~1.2 log units for the $H(\tau)$ peak attributed to bond scission/renewal dynamics is found to remain effectively constant for all [NaPO₃]_x[Zn(PO₃)₂]_{1-x} liquids, consistent with its assignment to a bond scission/renewal process.

The validity of the deconvolution of the $H(\tau)$ spectra into two relaxation processes can be assessed by a comparison between the average timescales for these two processes measured in this study with those reported by Sidebottom and Vu for the [NaPO₃]_{0.8}[Zn(PO₃)₂]_{0.2} liquid using photon correlation spectroscopy (PCS).²¹ Such a comparison is shown in Fig. 9. Sidebottom and Vu observed two dynamical processes in their study, the faster of which was characterized by a higher activation energy and was assigned to the shear relaxation, while the slower process with a lower activation energy was found to be a diffusive mode that was tentatively assigned to the slow diffusion of Zn atoms. It is clear from Fig. 9 that the relaxation time of fast chain dynamics obtained by oscillatory shear in the present study and that of fast dynamics reported by Sidebottom and Vu are in good agreement. Furthermore, these timescales are also in good agreement with the shear relaxation time for this liquid obtained from the Maxwell relation $\tau = \eta/G_{\infty}$, where η and G_{∞} were measured in the present study using steady shear rheometry and RUS, respectively. These results suggest that the shear relaxation of these metaphosphate liquids is controlled by segmental motion of the phosphate chains, the timescale distribution of which is represented by the broad peak at longer timescale in the $H(\tau)$ spectra in Fig. 6. On the other hand, the timescale corresponding to the slow bond scission/renewal dynamics in the [NaPO₃]_{0.8}[Zn(PO₃)₂]_{0.2} liquid as observed in the

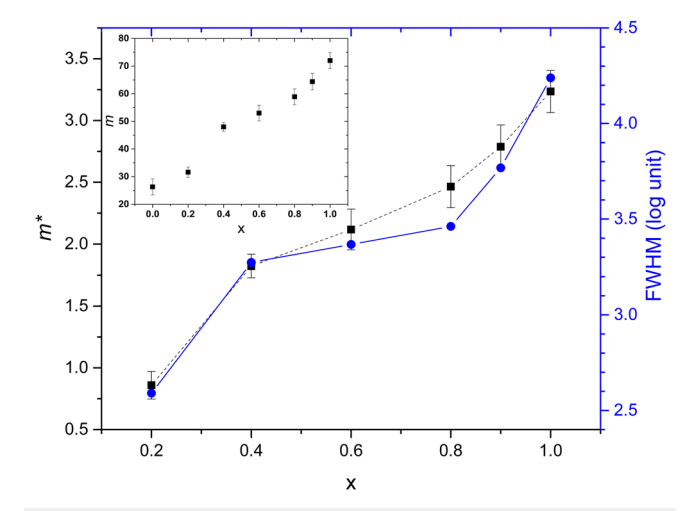


FIG. 8. Compositional dependence of reduced fragility indices of $[NaPO_3]_x[Zn(PO_3)_2]_{1-x}$ supercooled liquids obtained in the present study (black square) and of FWHM of the Gaussian component corresponding to segmental chain motion in the relaxation spectra $H(\tau)$ (blue circle). Dashed lines are a guide to the eye. The inset shows corresponding compositional variation of the fragility indices of these liquids.

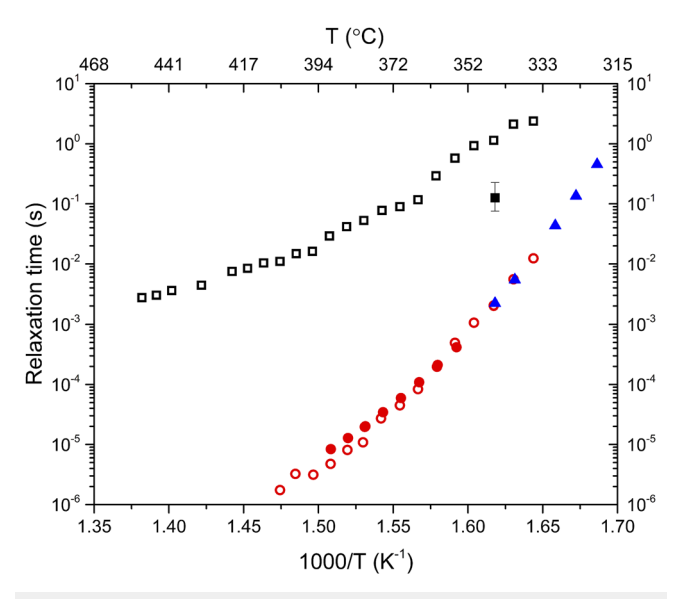


FIG. 9. Temperature dependence of the Maxwell relaxation timescale from viscosity data (filled red circles) and relaxation timescale of the fast (filled blue triangles) and slow (filled black square) dynamical processes obtained from oscillatory shear rheometry in the present study for the [NaPO₃]_{0.8}[Zn(PO₃)₂]_{0.2} liquid. The relaxation time of slow process (open black square) and fast process (open red circle) for this liquid obtained using PCS in a previous study are shown for comparison.²¹

 $H(\tau)$ spectrum is consistent with, albeit somewhat faster than, the timescale of the slow process reported by Sidebottom and Vu using PCS (Fig. 9). However, the observed discrepancy in the timescales measured by SAOS rheometry in the present study and by PCS in Ref. 21 can be related to the fact that this timescale was observed in the PCS measurements to be strongly dependent on the scattering wavevector q. It is important to note here that the assignment of the slow dynamics in the present study to Zn–O bond scission/renewal is consistent with Sidebottom and Vu's assignment of this process to Zn diffusion based on the q-dependence of its timescale. ²¹

IV. SUMMARY

All $[NaPO_3]_x[Zn(PO_3)_2]_{1-x}$ supercooled liquids display thermorheological complexity and the coexistence of two dynamical processes with timescales differing by nearly two orders of magnitude. The fast process, attributed to the segmental motion of the constituent metaphosphate chains, is characterized by a broad timescale distribution, and it predominantly controls the shear relaxation process in these liquids. On the other hand, the slow process can be ascribed to the diffusive Zn–O bond scission/renewal dynamics. The kinetic fragility index of these liquids monotonically increases with the increasing Na:Zn ratio and is shown to be correlated with the conformational entropy of the metaphosphate chains. This conformational entropy is hypothesized to be a function of the degree of effective inter-chain cross-linking, which increases with the increasing Zn content, imparted by the modifier–oxygen coordination polyhedra.

ACKNOWLEDGMENTS

This work was supported by a grant from the National Science Foundation (Grant No. NSF-DMR 1855176) to S.S.

DATA AVAILABILITY

The data that support the findings of this study are available from the corresponding author upon reasonable request.

REFERENCES

¹R. K. Brow, J. Non-Cryst. Solids **263-264**, 1 (2000).

²E. H. Oelkers and J.-M. Montel, Elements 4, 113 (2008).

³P. Y. Shih, Mater. Chem. Phys. **80**, 299 (2003).

⁴J. A. Wilder, J. Non-Cryst. Solids **38-39**, 879 (1980).

⁵L. L. Hench, R. J. Splinter, W. C. Allen, and T. K. Greenlee, J. Biomed. Mater. Res. 5, 117 (1971).

⁶C. Bergmann, M. Lindner, W. Zhang, K. Koczur, A. Kirsten, R. Telle, and H. Fischer, J. Eur. Ceram. Soc. **30**, 2563 (2010).

⁷C. Hönninger, F. Morier-Genoud, M. Moser, U. Keller, L. R. Brovelli, and C. Harder, Opt. Lett. **23**, 126 (1998).

⁸N. G. Boetti, D. Pugliese, E. Ceci-Ginistrelli, J. Lousteau, D. Janner, and D. Milanese, Appl. Sci. 7, 1295 (2017).

⁹D. Pugliese, N. G. Boetti, J. Lousteau, E. Ceci-Ginistrelli, E. Bertone, F. Geobaldo, and D. Milanese, J. Alloys Compd. **657**, 678 (2016).

¹⁰F. Muñoz, J. Rocherullé, I. Ahmed, and L. Hu, Springer Handbook of Glass (Springer, Cham, 2019), pp. 553–594.

¹¹ R. K. Brow, T. M. Alam, D. R. Tallant, and R. J. Kirkpatrick, MRS Bull. 23, 63 (1998).

¹²J.-J. Liang, R. T. Cygan, and T. M. Alam, J. Non-Cryst. Solids **263-264**, 167 (2000).

¹³Y. Onodera, S. Kohara, H. Masai, A. Koreeda, S. Okamura, and T. Ohkubo, Nat. Commun. 8, 15449 (2017).

¹⁴L. Y. Zhang, H. Li, and L. L. Hu, J. Alloys Compd. 734, 163 (2018).

¹⁵S. Yan, Y. Yue, Y. Wang, Y. Diao, D. Chen, and L. Zhang, J. Non-Cryst. Solids 520, 119455 (2019).

¹⁶B. G. Aitken, S. C. Currie, B. C. Monahan, L. Wu, and E. W. Coonan, U.S. patent 7116888 (3 October 2006).

¹⁷D. L. Sidebottom, T. D. Tran, and S. E. Schnell, J. Non-Cryst. Solids 402, 16 (2014).

¹⁸D. L. Sidebottom, Phys. Rev. E **92**, 062804 (2015).

¹⁹Y. Xia, W. Zhu, M. Lockhart, B. Aitken, and S. Sen, J. Non-Cryst. Solids **514**, 77 (2019)

²⁰L. Muñoz-Senovilla and F. Muñoz, J. Non-Cryst. Solids 385, 9 (2014).

²¹ D. L. Sidebottom and D. Vu, J. Chem. Phys. **145**, 164503 (2016).

²²Y. Xia, W. Zhu, J. Sen, and S. Sen, J. Chem. Phys. **152**, 044502 (2020).

 $^{\bf 23}$ S. Wegner, L. van Wüllen, and G. Tricot, J. Phys. Chem. B 113, 416 (2009).

²⁴S. Sen, Prog. Nucl. Magn. Reson. Spectrosc. **116**, 155 (2020).

²⁵W. Zhu, B. Aitken, and S. Sen, J. Non-Cryst. Solids **534**, 119959 (2020).

²⁶W. Zhu, M. Lockhart, B. Aitken, and S. Sen, J. Non-Cryst. Solids **502**, 244 (2018).

 $^{\bf 27}$ R. L. Sammler, J. U. Otaigbe, M. L. Lapham, N. L. Bradley, B. C. Monahan, and C. J. Quinn, J. Rheol. $\bf 40,$ 285 (1996).

²⁸S. Wei, G. J. Coleman, P. Lucas, and C. A. Angell, Phys. Rev. Appl. 7, 034035 (2017).

²⁹Y. Xia, B. Yuan, O. Gulbiten, B. Aitken, and S. Sen, J. Phys. Chem. B **125**, 2754 (2021).

³⁰ F. F. Balakirev, S. M. Ennaceur, R. J. Migliori, B. Maiorov, and A. Migliori, Rev. Sci. Instrum. 90, 121401 (2019).

³¹ A. Migliori, J. L. Sarrao, W. M. Visscher, T. M. Bell, M. Lei, Z. Fisk, and R. G. Leisure, Physica B **183**, 1 (1993).

³²O.-V. Laukkanen, Rheol. Acta **56**, 661 (2017).

- ³³ N. V. Pogodina, M. Nowak, J. Läuger, C. O. Klein, M. Wilhelm, and C. Friedrich, J. Rheol. 55, 241 (2011).
- 34 S. Sen, W. Zhu, and B. G. Aitken, J. Chem. Phys. 147, 034503 (2017).
- ³⁵W. Zhu, B. Aitken, and S. Sen, J. Non-Cryst. Solids **478**, 79 (2017).
- ³⁶C. Gainaru, R. Figuli, T. Hecksher, B. Jakobsen, J. C. Dyre, M. Wilhelm, and R. Böhmer, Phys. Rev. Lett. **112**, 098301 (2014).
- ³⁷N. Lou, Y. Wang, X. Li, H. Li, P. Wang, C. Wesdemiotis, A. P. Sokolov, and H. Xiong, Macromolecules 46, 3160 (2013).
- ³⁸S. Trinkle and C. Friedrich, Rheol. Acta **40**, 322 (2001).
- ³⁹J. D. Ferry, Viscoelastic Properties of Polymers (John Wiley & Sons, 1980).
- ⁴⁰ W. Zhu, B. G. Aitken, and S. Sen, J. Chem. Phys. **150**, 094502 (2019).
- ⁴¹B. Yuan, B. Aitken, and S. Sen, J. Non-Cryst. Solids **559**, 120669 (2021).

- ⁴² M. Crobu, A. Rossi, F. Mangolini, and N. D. Spencer, Anal. Bioanal. Chem. 403, 1415 (2012).
- ⁴³ J. W. Wiench, M. Pruski, B. Tischendorf, J. U. Otaigbe, and B. C. Sales, J. Non-Cryst. Solids **263-264**, 101 (2000).
- ⁴⁴L. Muñoz-Senovilla, S. Venkatachalam, F. Muñoz, and L. Van Wüllen, J. Non-Cryst. Solids 428, 54 (2015).
- ⁴⁵ H. A. S. Al-Shamiri and A. S. Eid, Photonics Optoelectron. **1**, 1 (2012).
- ⁴⁶ K. A. Matori, M. Hafiz, M. Zaid, H. J. Quah, S. Hj, A. Aziz, Z. A. Wahab, M. Sabri, and M. Ghazali, Adv. Mater. Sci. Eng. 2015, 596361.
- ⁴⁷P. K. Jha, O. P. Pandey, and K. Singh, J. Mol. Struct. **1083**, 278 (2015).
- ⁴⁸ Z. Černošek, M. Chládková, and J. Holubová, J. Non. Cryst. Solids **531**, 119866 (2020).
- ⁴⁹B. C. Tischendorf, T. M. Alam, R. T. Cygan, and J. U. Otaigbe, J. Non-Cryst. Solids **316**, 261 (2003).